

Flow Behavior and Aging of Pyrolysis Oils from Different Feedstocks

Leon Jampolski,^{*,†} Marco Tomasi Morgano,[‡] Helmut Seifert,[‡] Thomas Kolb,[§]
and Norbert Willenbacher[†]

[†]Applied Mechanics, Institute for Mechanical Process Engineering and Mechanics, Karlsruhe Institute of Technology, 76131 Karlsruhe, Germany

[‡]Pyrolysis/Gas Treatment, Institute for Technical Chemistry, Karlsruhe Institute of Technology, 76344 Eggenstein-Leopoldshafen, Germany

[§]Gasification Technology, Institute for Technical Chemistry, Karlsruhe Institute of Technology, 76344 Eggenstein-Leopoldshafen, Germany

Supporting Information

ABSTRACT: This work focuses on the flow behavior and accelerated aging of pyrolysis oils produced in a screw reactor from different feedstocks. Beech wood, wheat straw, chicken manure, and sewage sludge were pyrolyzed at 350, 400, 450, and 500 °C, and the viscosity of the corresponding oils was measured at four different temperatures between 20 and 80 °C, with values up to 1 Pa s at 20 °C. Newtonian flow behavior was observed, except for wheat straw pyrolysis oils at temperatures below 50 °C. Absolute viscosity values as well as flow activation energies (E_A), covering a range from 38 to 57 kJ mol⁻¹, turned out to be independent of the pyrolysis temperature, except for beech wood oil. In this latter case, a peak in viscosity and activation energy was found at a pyrolysis temperature of 450 °C and is attributed to the low water content of the oil obtained at this temperature. Accelerated aging experiments were conducted for 24 h at 40 and 80 °C. For the latter temperature, the effect of a free surface and an inert gas atmosphere on aging was examined. This enabled us to separate the effect of polymerization and evaporation of volatiles on the change in viscosity. In both cases, beech wood pyrolysis oil showed the strongest aging (~20-fold increase in viscosity). The lowest aging was found for wheat straw pyrolysis oil in a free surface sample cell, while almost no aging occurred under an inert gas atmosphere. Therefore, we conclude that aging of beech wood oil is mostly due to polymerization, whereas aging of wheat straw oil is essentially due to evaporation of volatiles. For chicken manure and sewage sludge oils, both polymerization and evaporation contribute almost equally to the increase of viscosity when an open sample cell is used. For beech wood pyrolysis oil, size-exclusion chromatography revealed a change in molecular weight upon aging from $M_w = 190$ to 240 Da. A slight increase in M_w could be detected for chicken manure and sewage sludge, but no indication for polymerization was found for wheat straw. Gas chromatography coupled with mass spectrometry was used to determine the concentration of characteristic oil components quantitatively, confirming the conclusions from viscosity measurements regarding aging mechanisms.

1. INTRODUCTION

Biomass pyrolysis is defined as a thermochemical process performed in the absence of oxygen at typical temperatures of 350–550 °C, where the lignocellulosic biomass is converted into solids (char/coke), gases, and liquids.^{1,2} One of the obtained liquids is called pyrolysis oil or bio-oil. It has a dark brown color and a pronounced smoky odor and consists of a large number of organic compounds.³ Those oils can be used as an alternative carbonaceous fuel in the future as well as a replacement or blending agent of abating fossil fuels in the field of transportation and gasification.^{4–6} Pyrolyzed biomass used as feed for gasification can be reformed into synthesis gas, with a subsequent gas cleaning using the Fischer–Tropsch process to produce synthetic fuels or hydrocarbons.^{7,8} Because many pyrolysis oils tend to become unstable or exhibit phase separation during storage,⁹ a lot of effort has been spent to upgrade and stabilize pyrolysis oils through catalysis.^{10–15} This catalytic treatment mostly improves the properties of the pyrolysis oils, but it is sophisticated, time-consuming, and, therefore, expensive. Whether such a catalytic stabilization is necessary has to be examined for each oil individually. The flow

behavior of pyrolysis oils is a key parameter for handling and processing¹⁶ and has motivated this broadly based study on viscosity of such oils, including the effect of aging.

Previously, Chaala et al. performed thermal stability tests measuring the variation in viscosity, molecular weight distribution, and water content of different wood-based pyrolysis oils at increased temperatures for certain time periods with a spindle in cup viscometer. An increase of the viscosity was accompanied by a decrease of low-molecular-weight compounds, while the amount of high-molecular-weight compounds increased, indicating polymerization.¹⁷ Similar observations were reported by others, and polymerization turned out to be more pronounced at an increased aging temperature.^{18–20}

In all of the above-mentioned investigations, the viscosity was determined at only one shear rate and one temperature. Nolte and Liberatore²¹ investigated the viscosity of oils from different

Received: January 18, 2017

Revised: March 27, 2017

Published: March 30, 2017



feedstocks as a function of the shear rate at various temperatures. Viscosity values in the range of 15–400 mPa s were obtained at 25 °C; viscosity values in the range of 10–130 mPa s were obtained at 40 °C; and viscosity values in the range of 5–50 mPa s were obtained at 55 °C, always determined at a shear rate of 100 s⁻¹.²¹ A correlation between viscosity and feedstock origin was not discussed. The covered viscosity range decreased with an increasing temperature, confirmed in an earlier work.¹⁸ Wood-based oils were found to be non-Newtonian at low temperatures, and oils from switch grass and wheat straw turned out to be biphasic and shear thinning in the whole investigated temperature range. Zhang et al. showed that biochar acts as a catalyst and boosts reactions within the pyrolysis oil, resulting in an increased water content and, thus, a decreased viscosity in the examined shear rate range from 100 to 500 s⁻¹.²² Furthermore, investigations of the flow behavior of blends of pyrolysis oil, char, and additives were performed, showing a viscosity reduction as a result of those additives.²³

In contrast to previous studies, Nolte and Liberatore used a sealed pressure cell in a rheometer for the *in situ* measurements of the viscosity during accelerated aging and confirmed that this procedure yields similar results as common aging experiments, where viscosity measurements are performed after different storage times.²⁴ The treatment of a pyrolysis oil sample at 80 °C for 24 h in a tightly sealed container was found to be equivalent to an aging of the oil for approximately 1 year at room temperature in a sealed reservoir.²⁵

This work focuses on the flow properties of oils from four different feedstocks (beech wood, wheat straw, sewage sludge, and chicken manure) pyrolyzed at 350, 400, 450, and 500 °C, and their aging behavior. Rotational rheometer measurements were conducted at different temperatures. The effect of polymerization and evaporation of volatiles on the aging of pyrolysis oils from different feedstocks was examined. Aging experiments were performed using an open sample cell as well as a sealed pressure cell similar to the cell used by Nolte and Liberatore, providing an inert gas atmosphere. In contrast, we used a double-wall concentric cylinder system instead of a regular coquette cell, providing higher torque sensitivity. Viscosity measurements characterizing aging were complemented by size-exclusion chromatography (SEC) and gas chromatography coupled with mass spectroscopy (GC-MS) to disclose the dominating aging mechanisms.

2. MATERIALS AND METHODS

2.1. Materials. Pyrolysis oils were produced using an intermediate pyrolysis trough screw reactor called STYX, which integrates hot gas filtration within the reactor vessel as a vapor pre-condition step that is known to have a stabilizing effect on the oil.^{26–28} This reactor measures approximately 2 m in heated length, has a diameter of 0.15 m, and is divided into seven segments. The feed has a well-defined residence time in the reactor by adjusting the rotational speed of the screw. Temperatures between 350 and 550 °C can be regulated with external independent electrical heaters. A particle and ash-free oil is obtained by recovering desired substances at different positions along the reactor.²⁹ Four different feedstocks were pyrolyzed at 350, 400, 450, and 500 °C at mass flows between 2 and 4 kg h⁻¹. Beech wood (BW) and wheat straw (WS) were included in this study as lignocellulosic biomass as well as sewage sludge (SS) and chicken manure (CM) as the biogenic residues from zoomass. The density ρ of the obtained oils was measured using a pycnometer after Gay-Lussac with a volume of 10.210 mL (Carl Roth GmbH, Karlsruhe, Germany), and the surface tension Γ was obtained using a customized setup based on the pendant drop principle³⁰ with a needle diameter of 1.65 mm. These values are summarized in Table 1.

Table 1. Pyrolysis Oil Feedstocks, Corresponding Pyrolysis Temperature, Density, Surface Tension, and Mass Flow

feedstock	pyrolysis temperature T_{pyro} (°C)	density, ρ (g cm ⁻³)	surface tension, Γ (mN m ⁻¹)	mass flow (kg h ⁻¹)
beech wood (BW)	350	1.155 ± 0.001	35.1 ± 0.1	2
	400	1.163 ± 0.003	35.5 ± 0.1	2
	450	1.179 ± 0.003	36.1 ± 0.1	2
	500	1.156 ± 0.001	35.6 ± 0.1	2
wheat straw (WS)	350	1.092 ± 0.001	28.8 ± 1.0	3
	400	1.098 ± 0.001	26.6 ± 2.2	3
	450	1.108 ± 0.003	25.7 ± 0.8	3
	500	1.069 ± 0.004	22.6 ± 1.1	3
chicken manure (CM)	350	1.043 ± 0.001	31.7 ± 1.3	4
	400	1.039 ± 0.003	29.1 ± 0.7	4
	450	1.044 ± 0.006	32.4 ± 0.1	4
	500	1.050 ± 0.001	32.5 ± 0.1	4
sewage sludge (SS)	350	1.000 ± 0.001	28.5 ± 0.1	4
	400	1.004 ± 0.002	28.5 ± 0.1	4
	450	0.998 ± 0.001	28.4 ± 0.1	4
	500	1.026 ± 0.002	28.6 ± 0.2	4

2.2. Rheological Measurements. **2.2.1. Shear-Rate-Dependent Viscosity.** The rheological properties of the pyrolysis oils were characterized through the shear-rate-dependent viscosity η . Measurements were performed using a rotational rheometer (Physica MCR501, Anton Paar GmbH, Graz, Austria) equipped with a coaxial cylinder geometry (inner diameter, 26.66 mm; outer diameter, 28.92 mm). These measurements were conducted using a shear rate ramp (initial shear rate, 0.1 s⁻¹; final shear rate, 1000 s⁻¹), holding the shear rate for 20 s before recording the shear stress and calculating the corresponding viscosity. Preliminary experiments on WS pyrolysis oil revealed that this was sufficient to reach the steady state for each measuring point. The shear rate ramp was carried out at temperatures of 20, 40, 60, and 80 °C, and the WS produced at $T_{\text{pyro}} = 450$ °C was additionally measured at 50 °C. Viscosity measurements at high temperatures and low shear rates were limited by the torque resolution of the rheometer. Data access at high shear rates and low viscosity was limited presumably as a result of the formation of Taylor vortices indicated by an unexpected increase of viscosity at high shear rates.

The Arrhenius equation (eq 1) was used to calculate the flow activation energy E_A

$$\frac{\eta(T)}{\eta(T_0)} = \exp \left(\frac{E_A}{R} \left(\frac{1}{T} - \frac{1}{T_0} \right) \right) \quad (1)$$

where R is the ideal gas constant, $\eta(T)$ is the viscosity at the temperature T , and $\eta(T_0)$ is the viscosity at a reference temperature T_0 .

2.2.2. Aging under Shear. When pyrolysis oil shows an increase in viscosity after or during heating over time, this phenomenon is termed “aging”.^{3,18,20,24,31,32} To obtain insight into the aging behavior of the pyrolysis oil, samples were continuously sheared at a constant shear rate for 24 h at process relevant temperatures of 40 and 80 °C. Viscosity was recorded every 60 s. A coaxial cylinder sample cell geometry with a surface open to the atmosphere was used for these experiments, and a shear rate of 10 s⁻¹ was selected to mimic a pumping process. Secondary flows could be neglected at this intermediate shear rate. The torque was sufficient, even for the sample with the lowest viscosity, to receive a stress signal from the rheometer. Measurements of the shear-rate-dependent viscosity after the aging procedure were performed as described in section 2.2.1.

A pressure cell from Anton Paar, shown in Figure 1, was used to perform viscosity measurements under an inert gas atmosphere (N₂ with 99.999% purity, Air Liquide SA, Paris, France). This avoids evaporation of volatiles, and the viscosity increase observed in these experiments can be attributed to polymerization reactions. This hermetically sealed concentric double-wall cylinder geometry (with a

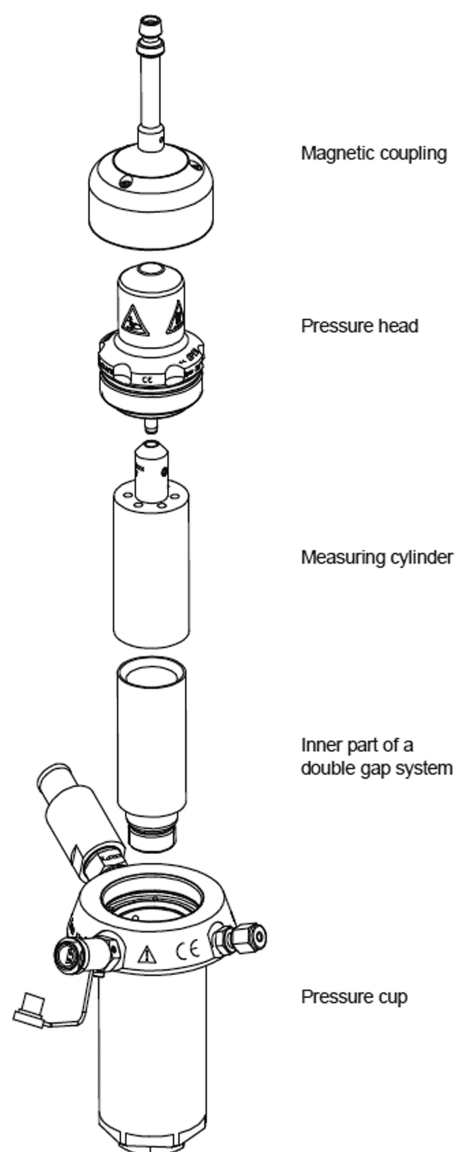


Figure 1. Scheme of the pressure cell setup (courtesy of Anton Paar).

gap width of 0.6 mm for both gaps) is specified for pressures up to 400 bar and temperatures up to 200 °C. Measurements were conducted at a shear rate of 10 s⁻¹, a temperature of 80 °C, and a constant pressure of 10 bar procured by a N₂ atmosphere. These real time viscosity measurements are similar to those described by Nolte and Liberatore.²⁴

2.3. Instrumental Analysis. The fresh pyrolysis oils were analyzed by means of elemental analysis as well as ash and water content according to the respective DIN standards. CHNO were determined using the German standard DIN EN 51732, where O was calculated by difference. Sulfur and chlorine were determined according to DIN EN 14582. The heating values were measured under the standard DIN 51900. Finally, the ash and water contents were determined according to DIN 51719 and DIN EN 14346, respectively (see Tables 2–5).

GC–MS was employed to identify the most relevant substances in the pyrolysis oils. The samples were shaken strongly and homogenized in an ultrasonic bath for about 10–15 min. Afterward, 10 mL of tetrahydrofuran (THF, SEC grade, Scharlau, Scharlab S.L., Barcelona, Spain) was used to dilute 1 g of pyrolysis oil. In the case of fresh and aged pyrolysis oils from lignocellulosic feedstocks, i.e., beech wood and wheat straw, isotope-marked internal standards of furfural, phenol, and guaiacol were added to each solution for a quantitative evaluation of these selected markers. The analysis were carried out adopting HP

Table 2. Elemental Composition of BW Oil Obtained at Different Pyrolysis Temperatures (T_{pyro}), Including the Ash and Water Contents

T_{pyro}	350 °C	400 °C	450 °C	500 °C
C (%)	49	51	54	55
H (%)	5	6	6	6
N (%)	0	0	0	0
O (%)	30	29	29	25
S (%)	0	0	0	0
water (%)	16	14	11	14
LHV (MJ kg ⁻¹)	21.0	21.1	22.3	22.6

Table 3. Elemental Composition of WS Oil Obtained at Different Pyrolysis Temperatures (T_{pyro}), Including the Ash and Water Contents

T_{pyro}	350 °C	400 °C	450 °C	500 °C
C (%)	50	58	53	56
H (%)	6	6	6	6
N (%)	1	1	1	2
O (%)	23	16	21	16
S (%)	0	0	0	0
water (%)	20	19	19	20
LHV (MJ kg ⁻¹)	20.8	23.3	22.3	23.4

Table 4. Elemental Composition of CM Oil Obtained at Different Pyrolysis Temperatures (T_{pyro}), Including the Ash and Water Contents

T_{pyro}	350 °C	400 °C	450 °C	500 °C
C (%)	67	53	61	54
H (%)	8	7	7	7
N (%)	5	6	7	9
O (%)	9	14	9	12
S (%)	0	1	1	1
water (%)	11	19	15	17
LHV (MJ kg ⁻¹)	31.4	22.3	27.9	26.5

Table 5. Elemental Composition of SS Oil Obtained at Different Pyrolysis Temperatures (T_{pyro}), Including the Ash and Water Contents

T_{pyro}	350 °C	400 °C	450 °C	500 °C
C (%)	57	65	64	65
H (%)	8	8	8	8
N (%)	6	7	8	8
O (%)	9	4	6	5
S (%)	1	1	1	1
water (%)	19	15	13	13
LHV (MJ kg ⁻¹)	28.0	28.9	28.3	30.2

6890 MSD; the column is a splitless Agilent CP-Wax 52 CB 60 m/0.32 mm inner diameter/0.25 μm film (Agilent Technologies, Santa Clara, CA, U.S.A.). Helium is used as the carrier gas. The profile of the oven temperature was the following: hold of 3 min at 45 °C, followed by a ramp of 3 °C min⁻¹ up to 180 °C. Then, the rate was increased to 7.5 °C min⁻¹ until 240 °C was reached.

The ash content was below the detection limit for BW, CM, and SS oils. Only for WS oil could an ash content of 0.1% be detected.

2.4. SEC. High-performance liquid chromatography (HPLC) was used to evaluate the occurrence of polymerization under accelerated aging conditions. Therefore, the pyrolysis oil was dissolved in THF with a concentration of 3 mg mL⁻¹ and filtered through 0.2 μm polytetrafluoroethylene (PTFE) membrane filters. SEC was performed

on HPLC (Agilent 1200 series, Agilent Technologies, Santa Clara, CA, U.S.A.) equipped with three polystyrene–divinylbenzene copolymer gel-packed columns (SDV LUX, 5 μm beads in a 5 \times 50 mm column and two 8 \times 300 mm columns) with nominal pore diameters of 10³, 10³, and 10⁵ Å (PSS Polymer Standards Service GmbH, Mainz, Germany). The THF flow rate was 1.0 mL min⁻¹, and the total injection volume was 100 μL . A calibration curve using polystyrene standards was applied to convert retention time into molecular weight. The molecular weight was calculated using the software provided by the manufacturer Agilent. These measurements were performed at the Institute for Chemical Technology and Polymer Chemistry at the Karlsruhe Institute of Technology (KIT).

3. RESULTS AND DISCUSSION

3.1. Flow Behavior. Viscosity data for oils from different feedstocks pyrolyzed at $T_{\text{pyro}} = 450$ °C were determined with rotational rheometry. At this pyrolysis temperature, the mass yield of oil from lignocellulosic feedstocks was largest compared to the other pyrolysis products (e.g., coke and aqueous condensate).³³ The viscosity of the BW, CM, and SS pyrolysis oils turned out to be independent of the shear rate at all investigated temperatures between 20 and 80 °C. Viscosity values for Newtonian oils (produced at $T_{\text{pyro}} = 450$ °C) are displayed in Table 6, with corresponding flow curves shown in

Table 6. Newtonian Viscosity Values of BW, WS, CM, and SS Produced at $T_{\text{pyro}} = 450$ °C at Temperatures between 20 and 80 °C

feedstock	measuring temperature (°C)	viscosity (mPa s)
beech wood (BW)	20	187
	40	44
	60	16
	80	7.5
wheat straw (WS)	60	13
	80	7
chicken manure (CM)	20	760
	40	161
	60	54
	80	22
sewage sludge (SS)	20	141
	40	40
	60	16
	80	8

the Supporting Information. The viscosity of BW oil decreases from 187 mPa s at 20 °C to 7.5 mPa s at 80 °C. For CM, the viscosity decreases from 760 mPa s at 20° to 22 mPa s at 80 °C. SS oil viscosity varies between 141 mPa s at 20 °C and 8 mPa s at 80 °C. Flow curves for WS pyrolysis oil are shown in Figure 2.

Non-Newtonian flow behavior is observed at temperatures up to 50 °C. This might be caused by the high amount of lignin-derived substances, such as phenol and guaiacol, present in this oil, as shown in Figure 7. These substances melt around 50 °C, and at $T \leq 50$ °C, probably a sample-spanning network exists formed of small crystals, resulting finally in the observed strong shear thinning. Moreover, phase separation was observed for shear rates above 100 s⁻¹. However, Newtonian flow behavior adjusts for temperatures above 50 °C for this sample, and the viscosity drops to 7 mPa s at 80 °C, similar to that for BW oil. In summary, independent of the feedstock, Newtonian flow behavior is found at temperatures ≥ 60 °C and the absolute viscosity values at

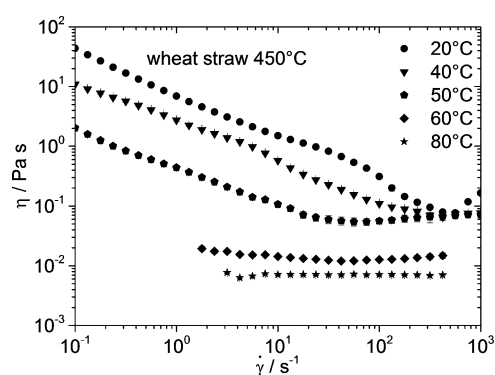


Figure 2. Flow curves of WS pyrolysis oil at 20 °C (circle), 40 °C (triangle), 50 °C (pentagon), 60 °C (diamond), and 80 °C (star) pyrolyzed at a temperature of 450 °C.

those temperatures are quite similar, except for the CM pyrolysis oil, which exhibits a ~ 3 times higher viscosity than the other oils investigated here.

3.2. Temperature Dependency. The viscosity at a shear rate of $\dot{\gamma} = 100$ s⁻¹ was considered for determination of the flow activation energy E_A because the WS oil exhibits shear thinning behavior at lower shear rates for $T < 50$ °C. The effect of the pyrolysis temperature (T_{pyro}) on the viscosity of the resulting oils is shown in Figure 3. To determine E_A , viscosity values for the different pyrolysis oils at 20, 40, 60, and 80 °C at $\dot{\gamma} = 100$ s⁻¹ are plotted over reciprocal absolute temperature, multiplied by 1000, and E_A is calculated according to eq 1, as described in section 2.2.1. E_A characterizes the dependency of viscosity on the temperature and can be related to the energy of vaporization.³⁴ Figure 3a clearly shows that BW oil obtained at $T_{\text{pyro}} = 450$ °C exhibits a maximum viscosity as well as activation energy. This may be due to the water content, which is at a minimum for the oil obtained at this pyrolysis temperature (see Table 2). Similar findings have been reported for oak pyrolysis oil.²¹ The reason for this variation in the water content is attributed to the thermal degradation of the essentially ash-free wood. Dehydration takes place for $T_{\text{pyro}} \leq 450$ °C, resulting in a decrease of the water content with increasing T_{pyro} up to 450 °C. This is followed by active and passive pyrolysis for higher temperatures,³⁵ and secondary gas-phase reactions become predominant in this temperature range, where an enhanced cracking of large compounds is also promoted by hot-gas filtration at such high temperatures. In combination with the further heterogeneous cracking at the surface of the filter, the presence of species with a higher molecular weight is reduced and the water content increases again, finally resulting in a maximum of viscosity and activation energy at $T_{\text{pyro}} = 450$ °C.

The water content of the second lignocellulosic pyrolysis product, namely, the WS oil, is independent of the pyrolysis temperature and slightly higher than that for the BW oil. In this case, non-Newtonian flow behavior is observed at low measuring temperatures, indicating a heterogeneous composition, and the simple Arrhenius-type temperature dependence of viscosity may not hold. We observe a large scatter in viscosity data (see Figure 3b) and no systematic trend with the pyrolysis temperature. Nevertheless, the whole set of $\eta(T)$ data was used to determine an apparent activation energy E_A .

Obviously, no systematic variation of absolute viscosity values or activation energy occurs for the oils from the zoomass feedstocks (see panels c and d of Figure 3). These results seem

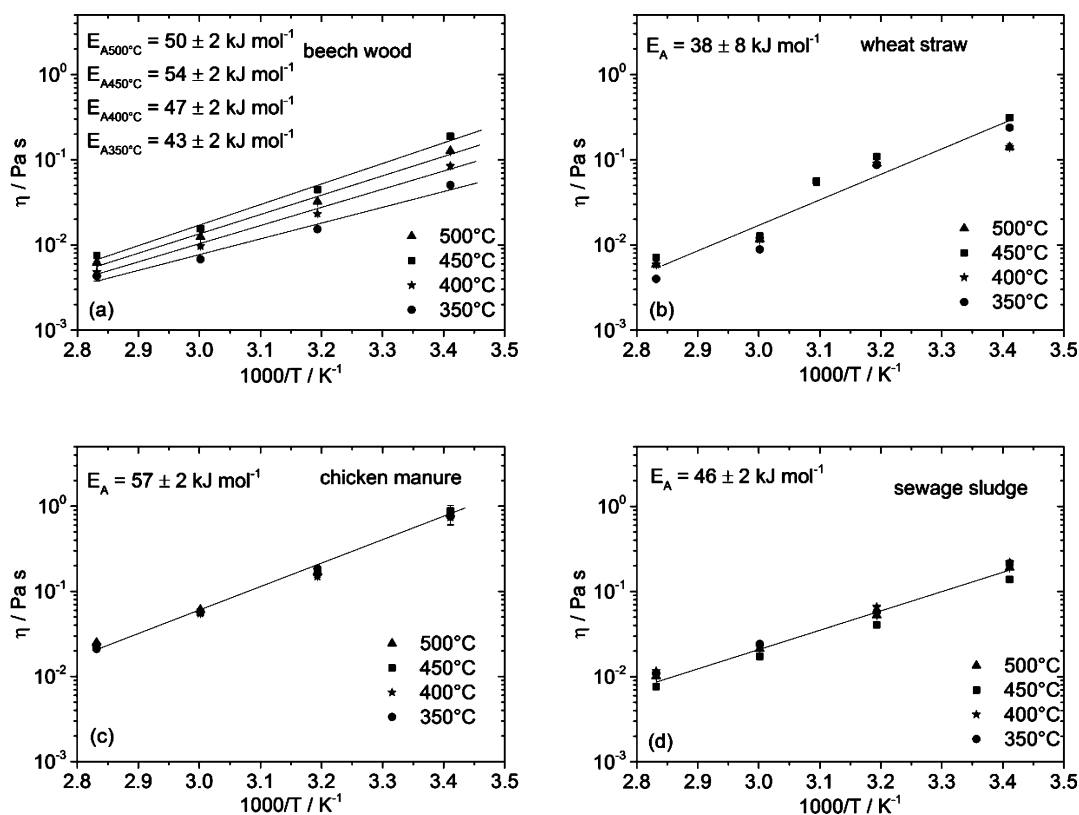


Figure 3. Viscosity at a shear rate of 100 s^{-1} over the reciprocal measuring temperature for oils obtained at different pyrolysis temperatures of $350 \text{ }^\circ\text{C}$ (circle), $400 \text{ }^\circ\text{C}$ (star), $450 \text{ }^\circ\text{C}$ (square), and $500 \text{ }^\circ\text{C}$ (triangle) of the following feedstocks: (a) BW, (b) WS, (c) CM, and (d) SS.

surprising because a variation in the water content is found similar to that for the BW oil. However, the oils from zoomass feedstocks include much more nitrogen than the lignocellulosic oils, providing the capability to bind water by hydrogen bridging.

The pyrolysis oil from CM not only exhibits the highest absolute viscosity values but also the strongest temperature dependence, resulting in $E_A = 57 \pm 2 \text{ kJ mol}^{-1}$. The lowest temperature dependence is found for WS pyrolysis oil, with $E_A = 38 \pm 8 \text{ kJ mol}^{-1}$, and the values found for SS and BW oils are in between.

3.3. Aging under a Free Surface. Viscosity is a key parameter for evaluation of processability and fuel quality. It affects fuel-pumping and combustion operations. Stability tests are usually performed at $80 \text{ }^\circ\text{C}$ for 24 h, measuring the absolute viscosity change over time. Such tests are called accelerated aging experiments.¹⁶ The change of viscosity is mainly associated with an increase in the molecular weight as a result of (phenolic) polymerization reactions, which are hastened at those conditions.¹⁸ Aging, however, can also be caused by evaporation of organic volatiles or water.^{15,18} Aging experiments have been performed under quiescent conditions as well as under shear.²⁴ In this work, we carried out aging experiments under shear, simulating a pumping process ($\dot{\gamma} = 10 \text{ s}^{-1}$) at 40 and $80 \text{ }^\circ\text{C}$ using a sample cell with a free surface as well as in a hermetically sealed pressure cell with an inert gas atmosphere at $80 \text{ }^\circ\text{C}$. This allows for a distinction between polymerization- and evaporation-controlled aging phenomena.

Figure 4 shows the viscosity increase after 10 and 24 h obtained from the sample cell with the free surface exemplary for samples produced at $T_{\text{pyro}} = 450 \text{ }^\circ\text{C}$. Data are normalized to the initial viscosity value for both temperatures. The first set of

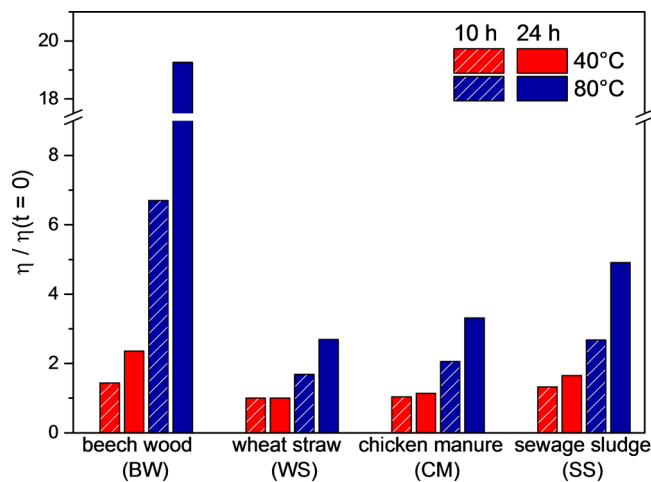


Figure 4. Viscosity data normalized to the respective initial value prior to aging $\eta(t=0)$ for BW, WS, CM, and SS at 10 h (diagonal pattern) and 24 h (no pattern) for $40 \text{ }^\circ\text{C}$ (red) and $80 \text{ }^\circ\text{C}$ (blue) with a constant shear rate of $\dot{\gamma} = 10 \text{ s}^{-1}$.

bars in Figure 4 displays the aging behavior of BW pyrolysis oil. The viscosity at $40 \text{ }^\circ\text{C}$ was ~ 1.4 and ~ 2.4 times higher than initially after 10 and 24 h of aging, respectively. An even more significant increase in viscosity by about a factor of 7 and 20 was observed at $80 \text{ }^\circ\text{C}$ for both time intervals. The second set of bars in Figure 4 shows the aging behavior of WS pyrolysis oil. At $40 \text{ }^\circ\text{C}$, almost no rise in viscosity occurs for the whole time range, but at $80 \text{ }^\circ\text{C}$, viscosity increases by a factor of ~ 1.7 after 10 h and then by ~ 2.7 after 24 h of aging. The viscosity values for CM are shown in the third set of bars in Figure 4. In this

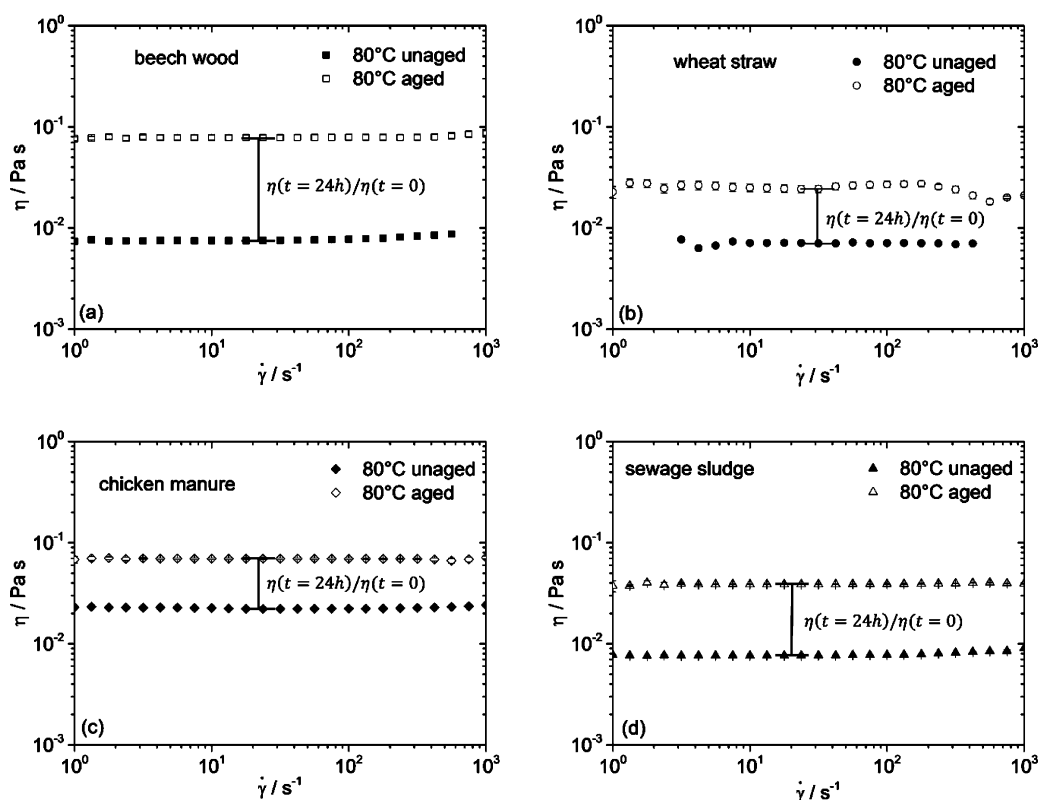


Figure 5. Flow curves of (a) BW, (b) WS, (c) CM, and (d) SS oils at 80 °C for the unaged (closed symbols) and aged (open symbols) samples. $\Delta\eta_{\text{aging}}$ is the viscosity increase during the accelerated aging experiment with a free surface sample cell.

case, no significant aging is observed at 40 °C; similar to wheat straw, the viscosity rises ~ 1.1 -fold at the end of the experiment. At 80 °C, a more distinct aging effect occurs with viscosity values ~ 2 and ~ 3.3 times that of the native oil for both time intervals. The last bar set of Figure 4 comprises the aging behavior of SS. $\eta/\eta(t=0)$ goes up to ~ 1.6 at 40 °C, and a value of ~ 4.9 is reached at 80 °C after 24 h of aging.

Obviously, BW oil has the most significant increase in viscosity in this accelerated aging experiment, followed by SS and CM, while WS is most stable under those aging conditions. For none of the examined particle-free pyrolysis oils did phase separation occur during the aging procedure. On the basis of Karl Fischer titration experiments, a water content below 1% is detected in the aged samples similar to that shown in previous studies.¹⁸ Additional weight measurements performed before and after aging revealed that the total loss of matter was in the range of the initial water content of the samples. Gravimetric measurements are not sensitive and accurate enough to detect the additional loss of apparently small fractions of organic volatiles.

Flow curve measurements (see section 3.1) performed for all investigated oils before and after aging confirmed that the flow behavior remains Newtonian, similar to that reported earlier.²⁴

The absolute increase in viscosity for BW oil is shown in Figure 5a, and corresponding data for WS oil are displayed in Figure 5b. Similar results were obtained for CM (Figure 5c) and SS (Figure 5d) oil. In all cases, flow behavior remains Newtonian even after accelerated aging. Note that the viscosity ratio $\eta(t=24\text{ h})/\eta(t=0)$ obtained in these experiments is in excellent agreement with the results shown in Figure 4. The deviation between these viscosity ratio values shown in Figures 4 and 5 is 2% for BW, CM, and SS oils but 10% for the WS oil.

3.4. Aging under an Inert Gas Atmosphere. A pressure cell similar to the cell used by Nolte and Liberatore²⁴ was used to avoid evaporation of volatiles. The setup is described in section 2.2.2. Aging was performed at $T = 80$ °C for 24 h, and viscosity was continuously recorded at a shear rate of $\dot{\gamma} = 10$ s⁻¹. Figure 6 displays corresponding results compared to those obtained using an open surface sample cell. For all investigated pyrolysis oils, the increase in viscosity under an inert gas atmosphere is significantly lower than with the free surface geometry, thus indicating that there is a contribution of volatile

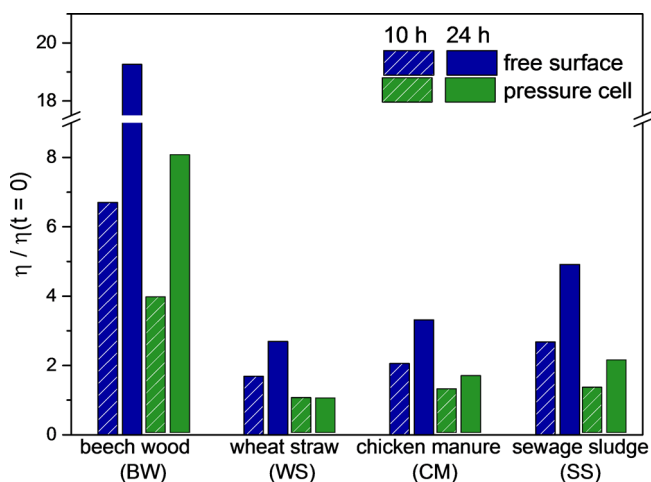


Figure 6. Viscosity data normalized to the respective initial value prior to aging $\eta(t=0)$ for BW, WS, CM, and SS at 10 h (diagonal pattern) and 24 h (no pattern) for an open surface (blue) and pressure cell (green) at 80 °C with a constant shear rate of $\dot{\gamma} = 10$ s⁻¹.

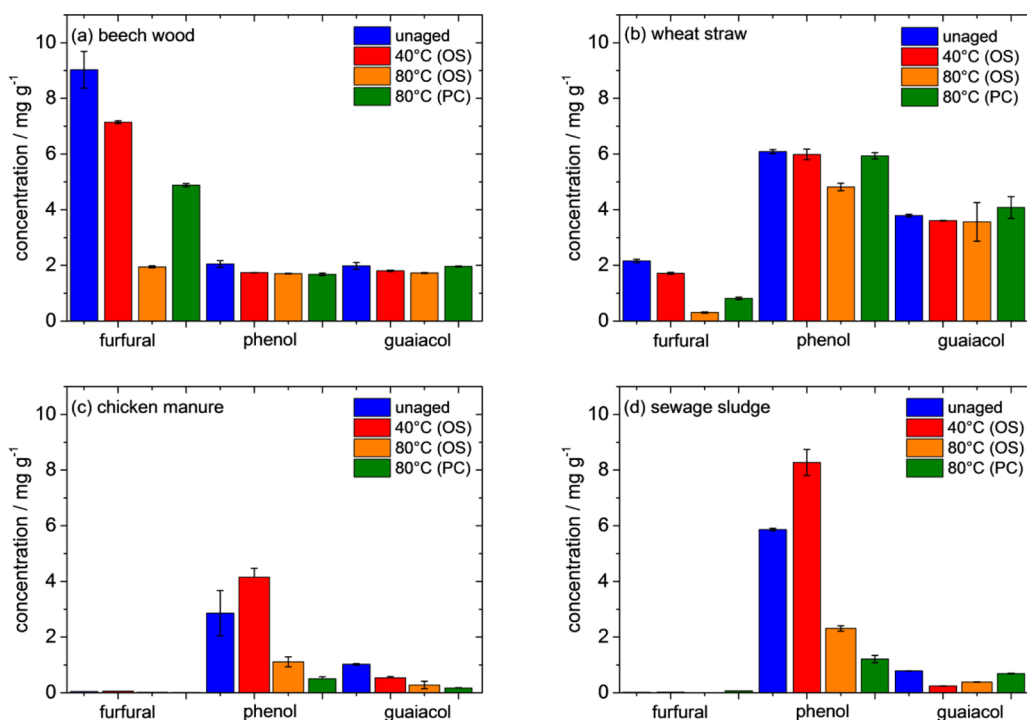


Figure 7. Concentration of furfural, phenol, and guaiacol in unaged (blue), open surface (OS) aged at 40 °C (red), OS aged at 80 °C (orange), and pressure cell (PC) aged at 80 °C (green) conditions of (a) BW, (b) WS, (c) CM, and (d) SS oils.

components to the observed viscosity increase for the free surface setup. The remaining increase in viscosity under an inert gas atmosphere is attributed to polymerization (or other chemical reactions).³⁶ As seen from the first set of bars in Figure 6, this polymerization is the major contribution to aging of BW oil.

In contrast, polymerization is insignificant, and the viscosity increase observed with the free surface system is solely due to evaporation of volatile compounds for the WS oil (second bar set in Figure 6), with the total increase in viscosity lowest in this case. Finally, for the CM and SS oils, evaporation and polymerization contribute equally to the viscosity increase observed using the free surface sample cell. Data documenting the full time evolution of viscosity during aging with an open surface as well as an inert gas atmosphere can be found in the Supporting Information.

3.5. GC–MS and SEC Analyses. Native and differently aged oils were analyzed with respect to their chemical composition using GC–MS and their molecular weight via SEC. A first qualitative analysis of the GC–MS results reveals an increase of the number and intensity of the peaks at the tail, above 50 min of retention time, comparing the aged samples to the native samples. Furfural, phenol, and guaiacol were measured quantitatively as markers of potentially ongoing reactions, with corresponding results shown in Figure 7.

The amount of phenol and guaiacol is much higher in the WS oil than in the BW oil. However, the furfural content in the BW oil is ~4 times that in the WS oil, but only a very small furfural content was detectable for the CM and SS oils as a result of their alkaline nature. The fraction of guaiacol in the oils from zoomass is substantially lower than in the oils from lignocellulosic feedstocks.

Aging at 40 °C has essentially no effect on the concentration of all three species in WS oil but leads to a slight reduction of these markers in BW oil. For the latter, aging at 80 °C results in

a drastic drop of the concentration for furfural but only in a slight decrease of phenol and guaiacol contents, regardless of whether an open surface or a sealed sample cell was used. Similarly, the concentration of these substances in WS oil drops when aged at 80 °C in an open surface sample cell. However, the concentration of phenol and guaiacol in WS oil remains constant upon aging at 80 °C in the pressure cell; only the furfural content seems to decrease under these conditions. This might be due to the systematic error resulting from the evaporation of the highly volatile substance during transfer of the sample from the pressure cell to the GC–MS device.

For the CM and SS oils, a rise of the phenol content during aging at 40 °C and a decrease during aging at 80 °C is found, which is more pronounced under an inert gas atmosphere than for the open surface conditions. The origin of this phenomenon remains unresolved because the chemistry in the presence of nitrogen (ions) is complex.³⁶ The guaiacol content of CM and SS oils is so small that a change of the relative content cannot be clarified considering the experimental uncertainty given here.

To confirm whether polymerization takes place during aging of these pyrolysis oils or not, SEC measurements were performed. An increase in the average molecular weight M_w from 190 to 240 Da is found for BW oil, indicating that the viscosity increase described above is partly due to polymerization, whereas no change in M_w is found for WS oil, which is in line with the viscosity data discussed above. For CM and SS oils, a weak increase in M_w (from 210 to 220 Da and from 190 to 200 Da, respectively) was found, indicating that polymerization may contribute to aging in these oils but to a lower extent than that in the BW oil.

Polymerization of BW oil may be due to furfural, which is present in the sample (see Figure 7) and has a strong tendency to polymerize as a result of its carbonyl group.³⁷ Polymerization or self-condensation could also be induced by olefin side groups of all lignin compounds in the oil.³⁸ The increase in M_w for BW

oil is in the same range as found for oak wood pyrolysis oil aged at 90 °C for 24 h.²⁴

In summary, these results suggest that polymerization-induced aging occurs in CM and SS oils but is most pronounced in BW oil. No indication for polymerization contribution to aging is found for WS oil. However, evaporation contributes to the viscosity increase during aging for all investigated oils.

4. CONCLUSION

We have investigated the flow behavior of pyrolysis oils from four different feedstocks (BW, WS, SS, and CM) pyrolyzed at 350, 400, 450, and 500 °C using coaxial cylinder rotational rheometry. Additionally, aging experiments were conducted with a free surface sample cell at 40 and 80 °C as well as in a hermetically sealed pressure cell with an inert gas atmosphere at 80 °C; in all cases, a shear rate of $\dot{\gamma} = 10 \text{ s}^{-1}$ was applied. With this setup, it was possible to distinguish between the influence of evaporation of organic volatiles or water and polymerization reactions on the viscosity increase during aging.

All investigated pyrolysis oils exhibit Newtonian flow behavior in the whole investigated temperature range between 20 and 80 °C, except for oil from WS, which exhibits strong shear thinning at temperatures of $T \leq 50 \text{ °C}$. This latter behavior may be attributed to residual phenolic crystals or aggregates forming a sample-spanning network structure. Oil from CM exhibits 3 times higher viscosity compared to the oils from BW, WS, and SS at temperatures of $T > 50 \text{ °C}$.

The pyrolysis temperature has essentially no effect on viscosity and its temperature dependence, except for BW oil. The temperature dependence of viscosity follows Arrhenius' law and is solely determined by the flow activation energy E_A . This quantity is highest for CM oil and lowest for WS oil. When BW is used as feedstock, absolute viscosity and E_A values are highest if pyrolysis is performed at $T_{\text{pyro}} = 450 \text{ °C}$, and this is presumably due to the low water content of the oil obtained at this temperature.

A substantial viscosity increase is observed during so-called accelerated aging experiments performed at 80 °C for BW and SS oil aging; i.e., an increase in viscosity is observed even during storage at 40 °C. This viscosity increase is most pronounced for BW oil and least for WS oil, and the viscosity increase for CM and SS oils is intermediate.

From a comparison of viscosity measurements performed using an open sample cell and a pressure cell providing an inert gas atmosphere, we conclude that aging of BW oil is mostly due to polymerization, whereas aging of WS oil is solely due to evaporation of volatiles. This is corroborated by GC–MS and SEC measurements. For CM and SS oils, both polymerization and evaporation contribute almost equally to the increase of viscosity when an open sample cell is used.

■ ASSOCIATED CONTENT

● Supporting Information

The Supporting Information is available free of charge on the ACS Publications website at DOI: 10.1021/acs.energyfuels.7b00196.

Flow curves of pyrolysis oils pyrolyzed at 450 °C, influence of pyrolysis properties on atomization, and continuous viscosity measurements during aging (PDF)

■ AUTHOR INFORMATION

Corresponding Author

*E-mail: leon.jampolski@kit.edu.

ORCID

Leon Jampolski: 0000-0001-5802-7650

Notes

The authors declare no competing financial interest.

■ ACKNOWLEDGMENTS

The authors thank the Helmholtz Association of German Research Centers (HGF) for partial funding of the work. Furthermore, the authors gratefully acknowledge Christoph Pfeifer from the Institute for Chemical Technology and Polymer Chemistry for performing the SEC measurements and Karim Abdel Aal for experimental support with rotational rheometry measurements. Additionally, the authors thank Tobias Jakobs for fruitful discussions.

■ REFERENCES

- (1) Bridgwater, A. V. An introduction to fast pyrolysis of biomass for fuels and chemicals. In *Fast Pyrolysis of Biomass: A Handbook*; CPL Scientific Publishing Services: Newbury, U.K., 1999; Vol 1, pp 1–13.
- (2) Bridgwater, A. V. Peacocke GVC. Fast pyrolysis processes for biomass. *Renewable Sustainable Energy Rev.* **2000**, *4* (1), 1–73.
- (3) Ortega, J. V.; Renehan, A. M.; Liberatore, M. W.; Herring, A. M. Physical and chemical characteristics of aging pyrolysis oils produced from hardwood and softwood feedstocks. *J. Anal. Appl. Pyrolysis* **2011**, *91* (1), 190–198.
- (4) Alonso, D. M.; Bond, J. Q.; Dumesic, J. A. Catalytic conversion of biomass to biofuels. *Green Chem.* **2010**, *12*, 1493–1513.
- (5) Higman, C.; van der Burgt, M. *Gasification*, 2nd ed.; Elsevier: Amsterdam, Netherlands, 2003.
- (6) Jiang, X.; Ellis, N. Upgrading bio-oil through emulsification with biodiesel: Thermal stability. *Energy Fuels* **2010**, *24* (4), 2699–2706.
- (7) Dahmen, N.; Henrich, E.; Dinjus, E.; Weirich, F. The bioliq® bioslurry gasification process for the production of biosynfuels, organic chemicals, and energy. *Energy Sustain Soc.* **2012**, *2* (1), 3.
- (8) Wright, M. M.; Brown, R. C.; Boateng, A. A. Distributed processing of biomass to bio-oil for subsequent production of Fischer–Tropsch liquids. *Biofuels, Bioprod. Biorefin.* **2008**, *2* (3), 229–238.
- (9) Oasmaa, A.; Kuoppala, E. Fast pyrolysis of forestry residue: Storage stability of liquid fuel. *Energy Fuels* **2003**, *17* (17), 1075–1084.
- (10) Zhang, Q.; Chang, J.; Wang, T. J.; Xu, Y. Upgrading bio-oil over different solid catalysts. *Energy Fuels* **2006**, *20* (6), 2717–2720.
- (11) Fisk, C. A.; Morgan, T.; Ji, Y.; Crocker, M.; Crofcheck, C.; Lewis, S. A. Bio-oil upgrading over platinum catalysts using in situ generated hydrogen. *Appl. Catal., A* **2009**, *358* (2), 150–156.
- (12) Widayatno, W. B.; Guan, G.; Rizkiana, J.; et al. Upgrading of bio-oil from biomass pyrolysis over Cu-modified β -zeolite catalyst with high selectivity and stability. *Appl. Catal., B* **2016**, *186*, 166–172.
- (13) Koike, N.; Hosokai, S.; Takagaki, A.; et al. Upgrading of pyrolysis bio-oil using nickel phosphide catalysts. *J. Catal.* **2016**, *333*, 115–126.
- (14) Xu, Y.; Wang, T.; Ma, L.; Zhang, Q.; Wang, L. Upgrading of liquid fuel from the vacuum pyrolysis of biomass over the Mo-Ni/ γ -Al₂O₃ catalysts. *Biomass Bioenergy* **2009**, *33* (8), 1030–1036.
- (15) Oh, S.; Choi, H. S.; Kim, U.-J.; Choi, I.-G.; Choi, J. W. Storage performance of bio-oil after hydrodeoxygenative upgrading with noble metal catalysts. *Fuel* **2016**, *182*, 154–160.
- (16) Yang, Z.; Kumar, A.; Huhnke, R. L. Review of recent developments to improve storage and transportation stability of bio-oil. *Renewable Sustainable Energy Rev.* **2015**, *50*, 859–870.
- (17) Chaala, A.; Ba, T.; Garcia-Perez, M.; Roy, C. Colloidal Properties of Bio-oils Obtained by Vacuum Pyrolysis of Softwood

Bark: Aging and Thermal Stability. *Energy Fuels* **2004**, *18* (3), 1535–1542.

(18) Diebold, J. P.; Czernik, S. Additives To Lower and Stabilize the Viscosity of Pyrolysis Oils during Storage. *Energy Fuels* **1997**, *11* (10), 1081–1091.

(19) Junming, X.; Jianchun, J.; Yunjuan, S.; Yanju, L. Bio-oil upgrading by means of ethyl ester production in reactive distillation to remove water and to improve storage and fuel characteristics. *Biomass Bioenergy* **2008**, *32* (11), 1056–1061.

(20) Alsbou, E.; Helleur, B. Accelerated aging of bio-oil from fast pyrolysis of hardwood. *Energy Fuels* **2014**, *28* (5), 3224–3235.

(21) Nolte, M. W.; Liberatore, M. W. Viscosity of biomass pyrolysis oils from various feedstocks. *Energy Fuels* **2010**, *24* (12), 6601–6608.

(22) Zhang, M.; Liaw, S. B.; Wu, H. Bioslurry as a fuel. 5. Fuel properties evolution and aging during bioslurry storage. *Energy Fuels* **2013**, *27* (12), 7560–7568.

(23) Gao, W.; Zhang, M.; Wu, H. Fuel properties and ageing of bioslurry prepared from glycerol/methanol/bio-oil blend and biochar. *Fuel* **2016**, *176*, 72–77.

(24) Nolte, M. W.; Liberatore, M. W. Real-Time Viscosity Measurements during the Accelerated Aging of Biomass Pyrolysis Oil. *Energy Fuels* **2011**, *25* (7), 3314–3317.

(25) Trinh, T. N.; Jensen, P. A.; Dam-Johansen, K.; Knudsen, N. O.; Sørensen, H. R.; Hvilsted, S. Comparison of lignin, macroalgae, wood, and straw fast pyrolysis. *Energy Fuels* **2013**, *27* (3), 1399–1409.

(26) Case, P. A.; Wheeler, M. C.; Desisto, W. J. Effect of residence time and hot gas filtration on the physical and chemical properties of pyrolysis oil. *Energy Fuels* **2014**, *28* (6), 3964–3969.

(27) Chen, T.; Wu, C.; Liu, R.; Fei, W.; Liu, S. Effect of hot vapor filtration on the characterization of bio-oil from rice husks with fast pyrolysis in a fluidized-bed reactor. *Bioresour. Technol.* **2011**, *102* (10), 6178–6185.

(28) Baldwin, R. M.; Feik, C. J. Bio-oil stabilization and upgrading by hot gas filtration. *Energy Fuels* **2013**, *27* (6), 3224–3238.

(29) Tomasi Morgano, M.; Leibold, H.; Richter, F.; Seifert, H. Screw pyrolysis with integrated sequential hot gas filtration. *J. Anal. Appl. Pyrolysis* **2015**, *113*, 216–224.

(30) Song, B.; Springer, J. Determination of Interfacial Tension from the Profile of a Pendant Drop Using Computer-Aided Image Processing. *J. Colloid Interface Sci.* **1996**, *184*, 77–91.

(31) Yu, F.; Deng, S.; Chen, P.; Liu, Y.; Wan, Y.; Olson, A.; Kittelson, D.; Ruan, R. Physical and Chemical Properties of Bio-Oils from Microwave Pyrolysis of Corn Stover. *Appl. Biochem. Biotechnol.* **2007**, *137–140* (1–12), 957–970.

(32) Oasmaa, A.; Peacocke, C. A guide to physical property characterisation of biomass-derived fast pyrolysis liquids. *VTT Publ.* **2001**, No. 450, 2–65.

(33) Oasmaa, A.; Fonts, I.; Pelaez-Samaniego, M. R.; Garcia-Perez, M. E.; Garcia-Perez, M. Pyrolysis Oil Multiphase Behavior and Phase Stability: A Review. *Energy Fuels* **2016**, *30* (8), 6179–6200.

(34) Glasstone, S.; Laidler, K. J.; Eyring, H. *The Theory of Rate Processes*; McGraw-Hill: New York, 1941.

(35) Słopiecka, K.; Bartocci, P.; Fantozzi, F. Thermogravimetric analysis and kinetic study of poplar wood pyrolysis. *Appl. Energy* **2012**, *97*, 491–497.

(36) Diebold, J. P. *A Review of the Chemical and Physical Mechanisms of the Storage Stability of Fast Pyrolysis Bio-oils*; National Renewable Energy Laboratory (NREL): Golden, CO, Jan 27, 1999; Technical Report NREL/SR-570-27613, DOI: [10.2172/753818](https://doi.org/10.2172/753818).

(37) Hu, X.; Wang, Y.; Mourant, D.; et al. Polymerization on Heating up of Bio-Oil: A Model Compound Study. *AIChE J.* **2013**, *59* (3), 888–900.

(38) Kim, T. S.; Kim, J. Y.; Kim, K. H.; et al. The effect of storage duration on bio-oil properties. *J. Anal. Appl. Pyrolysis* **2012**, *95*, 118–125.